RSC Advances

PAPER

View Article Online
View Journal | View Issue

Cite this: *RSC Adv.*, 2023, **13**, 17622

Polyacrylonitrile/UV329/titanium oxide composite nanofibrous membranes with enhanced UV protection and filtration performance†

Junlu Sheng,[ab] Shuiping Ding,[a] Haiyan Liao,[a] Yongbo Yao,*[a] Yunyun Zhai,[c] Jianchao Zhan[a] and Xueqin Wang*[d]

Ultraviolet (UV) radiation is extremely dangerous to humans and can contribute to immunosuppression, erythema, early ageing and skin cancer. UV protection finishing may greatly influence the handling and permeability of fabrics, while UV-proof fibres can guarantee close contact between UV-resistant agents and fabric without affecting the handling of the fabric. In this study, polyacrylonitrile (PAN)/UV absorber 329 (UV329)/titanium dioxide (TiO_2) composite nanofibrous membranes with complex, highly efficient UV resistance were fabricated *via* electrospinning. UV329 was included in the composite to further strengthen the UV resistance properties *via* absorption function, while TiO_2 inorganic nanoparticles were added to provide UV shielding function. The presence of UV329 and TiO_2 in the membranes was confirmed using Fourier-transform infrared spectroscopy, which also showed the absence of chemical bonds between PAN and the anti-UV agents. The PAN/UV329/TiO_2 membranes exhibited a UV protection factor of 1352 and a UVA transmittance of 0.6%, which indicate their extraordinary UV resistance properties. Additionally, filtration performance was investigated in order to expand the application field of the UV-resistant PAN/UV329/TiO_2 membranes, and the composite nanofibrous membranes showed a UV filtration efficiency of 99.57% and a pressure drop of 145 Pa. The proposed multi-functional nanofibrous membranes have broad application prospects in outdoor protective clothing and window air filters.

Received 13th April 2023
Accepted 30th May 2023

DOI: 10.1039/d3ra02470a

rsc.li/rsc-advances

Introduction

Because of the depletion of the stratospheric ozone layer, more ultraviolet (UV) light (100–400 nm) is now reaching the Earth.[1–4] Based on wavelength, UV radiation is classified into UVA (320–400 nm), UVB (280–320 nm) and UVC (200–280 nm).[5,6] In general, long-term exposure to UV radiation, especially the UVA and UVB components, can result in various skin conditions, such as skin damage, erythema, photo-ageing, immunosuppression and cancer.[7] To counteract these effects, anti-UV materials and methods have been developed. These are divided into two categories: UV-proof fibres and the UV protection finishing of fabrics.

UV protection finishing is based on coating fabrics with UV absorbing or blocking agents, which can effectively absorb UV light, greatly improving their UV protection performance. However, the finishing coating can significantly affect the handling and permeability of the fabric.[8–10] Instead, UV-proof fibres can be fabricated by mixing organic UV absorbers or inorganic UV shielding agents into a fibre-forming polymer solution before spinning, which can guarantee close contact between UV-proof agents and fibres.[11]

Among the developed UV-proof fibre preparation methods, electrospinning, which can produce, *via* easy processing, nanoscale fibres with a high specific surface area and high porosity, has attracted much attention.[12–15] Merati *et al.* fabricated electrospun polyacrylonitrile (PAN) nanofibrous mats embedded with zinc oxide (ZnO) nanoparticles and multi-walled carbon nanotubes; the composites with a 5 wt% ZnO content showed enough UV protection to meet standard requirements.[16] Moreover, nanofibres with a small diameter and high specific surface area can easily capture particles in the air and have better filtering efficiency for fine particles.[17] Moreover, window air

[a]*College of Materials and Textile Engineering, Nanotechnology Research Institute, Jiaxing University, Jiaxing 314001, China. E-mail: yaoyongbo@foxmail.com*
[b]*Key Laboratory of Yarn Materials Forming and Composite Processing Technology of Zhejiang Province, Jiaxing University, Jiaxing 314001, China*
[c]*Jiaxing Key Laboratory of Molecular Recognition and Sensing, College of Biological, Chemical Sciences and Engineering, Jiaxing University, Jiaxing 314001, China*
[d]*College of Textiles and Clothing, Qingdao University, Shandong 266071, China. E-mail: xqwang1989@163.com*

† Electronic supplementary information (ESI) available: UPF calculation and filtration performance test of the as-prepared membranes. FT-IR spectra of PAN, PAN/UV329-1, and PAN/UV329-1/TiO_2-0.5 nanofibrous membranes. Comparative analysis with the reported works. The average fibre diameter, mean pore diameter and filtration performance of PAN, PAN/UV329-1, and PAN/UV329-1/TiO_2-0.5 nanofibrous membranes. See DOI: https://doi.org/10.1039/d3ra02470a

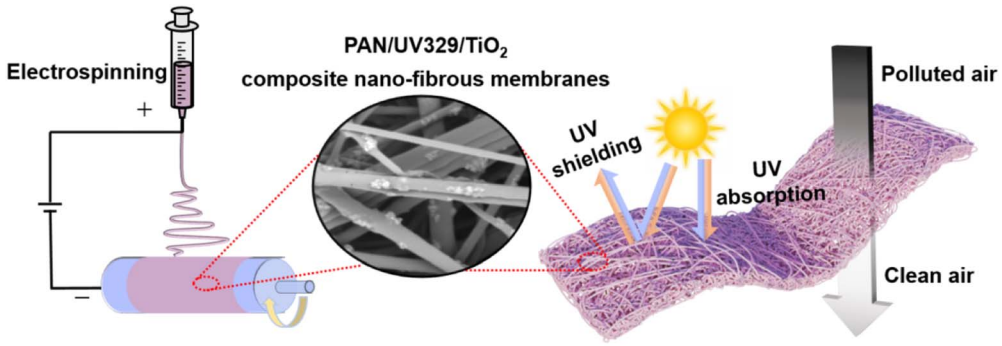

Fig. 1 Schematic showing the preparation of multifunctional PAN/UV329/TiO_2 composite nanofibrous membranes.

filters that maintain indoor air quality free from ultrafine particulate matter present in outdoor air require high UV resistance properties.[18] However, only a few studies have investigated the filtration performance of UV-proof nanofibrous membranes.

Herein, we propose a method for producing PAN nanofibrous membranes with enhanced UV protection properties that incorporate UV absorber 329 (UV329) and TiO_2 (Fig. 1). PAN was selected as the main polymer owing to its good elasticity, chemical stability, sunfast properties and excellent spinnability.[19] UV329, an organic UV absorber agent, was expertly inserted into the membranes *via* electrospinning to improve the UV resistance of the PAN/UV329 membranes. Further, different contents of TiO_2 nanoparticles were directly mixed with a PAN/UV329 solution. Owing to the double UV protective function of UV329 and TiO_2, the PAN-based nanofibrous membranes achieved high UV protection factor (UPF) values. In particular, to expand the applicability of the as-prepared membranes, we also studied their filtration properties.

Experimental

Materials

A powdered PAN (M_w = 90 000 g mol^{-1}) copolymer was purchased from Kaneka Co., Ltd, Japan. 2-(2-Hydroxy-5-*tert*-octylphenyl)benzotriazole (UV329) was supplied by Shandong Huaen Chemical Co., Ltd, China. TiO_2 (particle size = 5–10 nm) and *N*,*N*-dimethylacetamide (DMAc) were obtained from Sinopharm Chemical Reagent Co., Ltd, Shanghai, China. All reagents were used as purchased, without further purification.

Fabrication of PAN/UV329/TiO_2 nanofibrous membranes

First, a 10 wt% PAN homogeneous transparent solution was prepared by dissolving PAN in DMAc solvent *via* magnetic stirring for 12 h. Further, UV329 was blended with this 10 wt% PAN/DMAc solution at various contents (0, 0.5, 1, 2 and 4 wt%). After stirring for 12 h, homogeneous transparent solutions of PAN/UV329 were obtained and denoted as PAN/UV329-*x*, where *x* indicates the UV329 weight in wt%. Finally, with the PAN/UV329 content fixed at 1 wt%, we prepared PAN/UV329/TiO_2 electrospinning solutions containing different TiO_2 contents (0.1, 0.5, 1 and 2 wt%) by adding TiO_2 directly into the PAN/UV329 solutions. Before electrospinning, these colloidal mixtures were homogenised for 12 h with magnetic stirring and then set aside until no excess bubbles were present.

Regarding the electrospinning process, the as-prepared solutions were pumped through a capillary connected to a metal syringe needle in a DXES-3 electrospinning machine (Shanghai Oriental Flying Nano-Technology Co., Ltd, China); the feed rate was 1 mL h^{-1}, the applied voltage was 25 kV, the temperature was 25 ± 2 °C and the relative humidity was 50 ± 5%. The thickness of the membranes was approximately 23 ± 1 μm with a spinning time of about 4 h and all process parameters were kept constant. To explore the effects of the thickness on the UV protection and filtration performance of the PAN/UV329-1/TiO_2-0.5 composite nanofibrous membranes, the spinning time was regulated to acquire samples with different thicknesses. The spinning times were set as 1, 2, 3, 4, and 5 h, and as-prepared samples with different thicknesses of 6, 9, 11, 23, and 25 μm were acquired, respectively.

Characterisation and measurements

The surface morphology of the nanofibrous membranes was observed using a field emission scanning electron microscope (FE-SEM, Hitachi S-4800, Hitachi Ltd, Chiyoda-ku, Japan). The membranes were coated with gold using a sputtering technique prior to FE-SEM observation. The average diameters of the electrospun nanofibers were estimated from the SEM images using Adobe Acrobat 9.0 Professional, and at least 50 measurements were analyzed for each sample to obtain an average value. The diameter distributions were analyzed using the Origin Professional 9.0 software. A transmission electron microscopy (TEM) device (Talos F200X, Thermo Fisher Scientific, Czech Republic) was utilised to investigate the morphological structure of the membranes in more detail. The chemical structure and composition of the membranes were investigated using a Fourier-transform infrared (FTIR) spectrometer (Vertex 70, Bruker, Germany). The mean pore sizes of the as-prepared membranes were investigated using a CFP-1100AI instrument (Porous Materials Inc., USA) on the basis of a wet/dry flow method.

The tensile strength of the membranes was determined using an electronic tensile tester (Shanghai New Fibre Instrument Co., Ltd, Shanghai, China) at a tensile rate of 20 mm min^{-1}.

Rectangular samples with 30 × 3 mm dimensions were cut and clamped at their cut ends for testing. The samples were extended at a constant crosshead speed of 20 mm min^{-1} with a 10 mm gauge length. Every sample was tested at least three times to ensure reproducibility. The anti-UV performance was evaluated according to the UV reflection and absorption of the membranes by utilising a Labsphere UV-2000F UV transmittance analyser and a Cary 5000 UV-visible-near-infrared spectrophotometer, respectively. Every sample was tested in at least five different positions to ensure reproducibility. An automated filter tester provided by Huada Filter Technology Co., Ltd, China was used to measure the filtration efficiency and air-flow resistance of the membranes. The details of the UPF calculation and filtration performance testing listed in the ESI.†

Results and discussion

Effect of UV329 content

The morphologies of the PAN membranes blended with UV329 were investigated using FE-SEM, as shown in Fig. 2a–e. The nanofibres of the as-prepared membranes exhibited a smooth surface and the diameter distribution was uniform. As the UV329 content increased, the average diameter of the membranes gradually increased from 404 to 524 nm. This was caused by the increased viscosity of the electrospinning solution, which aided the entanglement of the molecular chains present in the membranes.[20]

The chemical bonds were investigated by comparing the FTIR spectra of original PAN membrane and PAN/UV329 nanofibrous membranes (Fig. 3). The peak detected at 2945 cm^{-1} was due to C–C skeleton vibrations. The peaks exhibited at 2242 and 1452 cm^{-1} by the pure PAN membranes were ascribed to C≡N and C–H vibrations, respectively.[21] The PAN/UV329 spectra showed the same characteristics as pure PAN, indicating that the UV329 addition did not change the chemical structure of PAN. Moreover, a peak was observed at 1519 cm^{-1} due to the C–H skeleton vibration of the benzenoid and other peaks appeared in the 900–653 cm^{-1} range (821, 800 and 752 cm^{-1}) as a result of C–H flexural vibrations of the substituted benzene ring.[22] A peak was detected at 1253 cm^{-1} due to C–O stretching vibrations. Moreover, the intensity of the

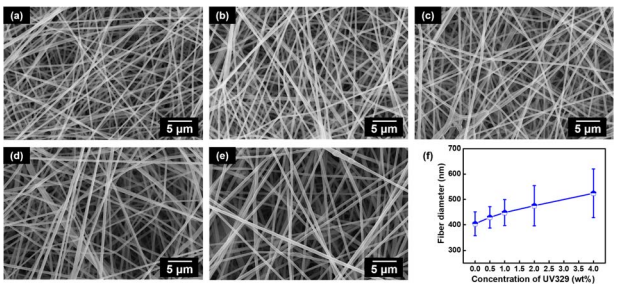

Fig. 2 (a)–(e) SEM images of PAN/UV329 composite nanofibrous membranes with different concentrations of UV329: (a) 0, (b) 0.5, (c) 1, (d) 2, and (e) 4 wt%. (f) Nanofibre diameter distribution of the relevant nanofibrous membranes.

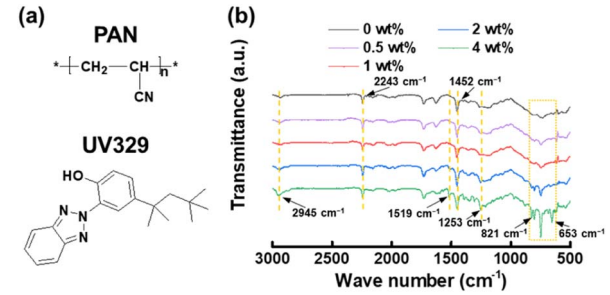

Fig. 3 (a) The chemical structural of PAN and UV329. (b) FTIR spectra of original PAN membrane and PAN/UV329 nanofibrous membranes with different concentrations of UV329.

transmission peaks increased with the UV329 content of the PAN/UV329 nanofibrous membranes.

The stress–strain curves of the pure PAN and PAN/UV329 nanofibrous membranes are shown in Fig. 4a. Regarding pure PAN, the tensile stress was 8.1 MPa and the elongation at break was 84.1%. After the addition of 0.5 wt% UV329, the stress increased to 8.6 MPa, while the elongation at break decreased to 62.9%. However, when further increasing the UV329 content, the mechanical performance of the membranes declined; the tensile stress and elongation at break were reduced to 3.6 MPa and 50.6%, respectively. This was likely due to the excessive addition of UV329 partly generating stress concentration and causing the asynchronism of the nanofiber fracture.[23–25] Moreover, the addition of small organic molecules into the PAN polymer matrix would damage the mechanical properties of the polymer materials.

The UV-blocking behaviour of the PAN/UV329 membranes was investigated by UV absorption spectroscopy (Fig. 4b). The pure PAN membranes exhibited virtually no absorption of UV radiation, particularly in the range of 280–400 nm. After introducing UV329, instead, the membranes showed broad

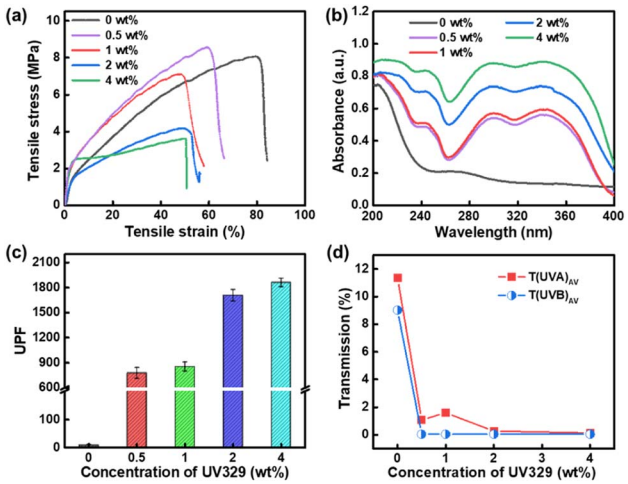

Fig. 4 Mechanical and UV protection performance of PAN/UV329 composite nanofibrous membranes with different concentrations of UV329: (a) stress–strain curves, (b) UV absorption spectra, (c) UPF value, and (d) $T(UVB)_{AV}$ and $T(UVA)_{AV}$.

absorption peaks at 240, 260 and 320 nm, indicating a wide UV resistance region. We attribute this to the UV absorption by UV329, which absorbed UV light that would have otherwise initiated photo-oxidation.[26,27]

The UPF is the ratio between the average effective UV irradiance on unprotected skin and that on protected skin; a value >50 indicates excellent UV protection.[28,29] Therefore, the UPF, UVA transmittance ($T(UVA)_{AV}$) and UVB transmittance ($T(UVB)_{AV}$) were measured to quantitatively analyse the UV protection performance of the PAN/UV329 membranes (Fig. 4c and d). The pure PAN membranes showed poor anti-UV performance, with a UPF of 10.3, $T(UVA)_{AV}$ of 11.4% and $T(UVB)_{AV}$ of 9.0%, which were lower than the requirements for real applications. Owing to the excellent UV absorption capacity of UV329, its addition significantly enhanced the membrane performance. The PAN/UV329-0.5 membranes increased to a UPF of 777 and a reduced $T(UVA)_{AV}$ of 1.1%. According to the Evaluation of UV Protection Performance of Textiles standard (GB/T 18830-2009), only products with UPF > 40.0 and $T(UVA)_{AV}$ < 5.0% can be referred to as UV protection products. Therefore, the PAN/UV329-0.5 membranes can be considered excellent UV-resistant textiles. When the concentration of UV329 was further increased to 1 wt%, the UPF improved to 854. PAN/UV329-4 exhibited even better anti-UV performance, with a UPF of 1862 and a $T(UVA)_{AV}$ of 0.1%. Focusing on the UV resistance of the membranes, PAN/UV329-1 was selected in the follow-up experiments to investigate the effect of TiO_2 on the morphological structure and properties of the membranes.

Effect of TiO_2 content

After fixing the UV329 content at 1 wt%, the effect of TiO_2 addition on the structure and mechanical behaviour of the membranes was also explored (Fig. 5 and 6). When the TiO_2 content was 0.1 wt%, the nanofibres overlapped with each other and were distributed evenly; the dispersion of TiO_2 nanoparticles within the nanofibres was verified through TEM. However, when further increasing the concentration of TiO_2 NPs from 0.5 to 2 wt%, the nanoparticles appeared outside the nanofibres and aggregated on their surface. As presented obviously in Fig. 6a, with increasing the addition amount of TiO_2 NPs, the average nanofibre diameter of the membranes increased from 500 to 703 nm.

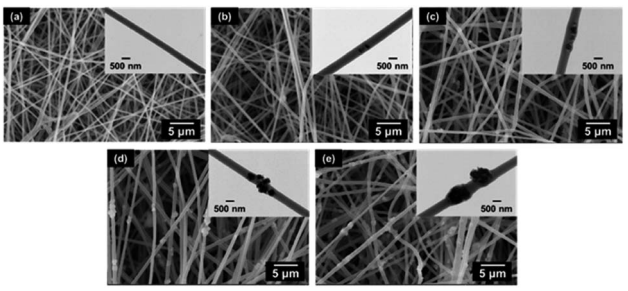

Fig. 5 (a)–(e) SEM and TEM images of PAN/UV329/TiO_2 composite nanofibrous membranes with different concentrations of TiO_2: (a) 0, (b) 0.1, (c) 0.5, (d) 1, and (e) 2 wt%.

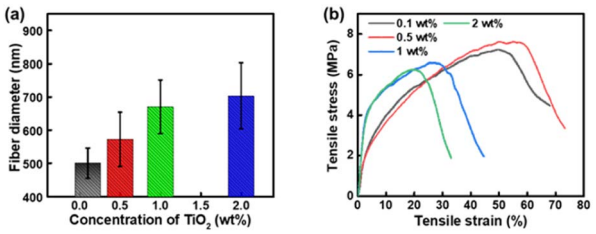

Fig. 6 (a) The nanofibre diameter and (b) stress–strain curves of the PAN/UV329/TiO_2 composite nanofibrous membranes with different concentrations of TiO_2.

TiO_2 nanoparticles were bonded with the PAN-based membranes *via* hydrogen bonding between –CN groups on the PAN polymer matrix and –OH groups on the TiO_2 nanoparticles.[30] The FT-IR spectra of the PAN, PAN/UV329-1, and PAN/UV329-1/TiO_2-0.5 membranes were shown in Fig. S1.† Considering the results from Fig. 3b and S1,† after the addition of TiO_2 nanoparticles at a concentration of 0.5 wt%, the intensity of the peaks at 736 and 611 cm^{-1} became stronger, which supported the presence of TiO_2 nanoparticles. Comparing these curves, new peaks were assigned to UV329 and TiO_2 composition, and there was no peak shift, which demonstrated that the obtained nanofibers possessed PAN, UV329, and TiO_2, and the three compounds did not exhibit any chemical interaction.

As shown in Fig. 4a and 6b, compared with the mechanical properties of the PAN/UV329-1 membranes, there was almost no change in those of the membrane with 0.1 wt% TiO_2. When the TiO_2 content was 0.5 wt%, the membrane achieved a tensile stress of 7.6 MPa and an elongation at break of 80.0%. The increase in the elongation at break was likely due to bits of nano-protrusions formed on the PAN/UV329/TiO_2 nanofibre surface that led to increased friction between the nanofibres. However, upon further increasing the TiO_2 content to 2 wt%, the tensile stress and elongation at break decreased to 6.2 MPa and 32.9%, respectively. These phenomena resulted from the excess incorporation of nanoparticles bringing about voids and inhomogeneity in the nanofibers, which destroyed the connections inside the nanofibers, leading to a decline in the mechanical properties.[31,32]

To investigate the effect of TiO_2 on the UV resistance of the as-prepared membranes, the UV absorption spectra, UPF, $T(UVA)_{AV}$ and $T(UVB)_{AV}$ of the PAN/UV329/TiO_2 membranes with different TiO_2 contents were also measured (Fig. 7a–c). Their UV absorption intensity decreased compared with that of the PAN/UV329-1 membrane. As the TiO_2 content increased, the $T(UVB)_{AV}$ was below 0.1%, while the $T(UVA)_{AV}$ ranged between 0.6% and 1.0%. The TiO_2 nanoparticles imparted the membranes with efficient UV scattering due to their large refractive index.[33,34] The UPF of the PAN/UV329-1 membranes was 854. After adding 0.1 wt% TiO_2, the UPF reached 1158, confirming that the anti-UV properties can be improved significantly through TiO_2 doping. The membrane with 0.5 wt% TiO_2 exhibited the best UV protection performance, with a UPF of 1352. When the TiO_2 content was further increased, the UPF declined. These findings reveal that the UV shielding properties

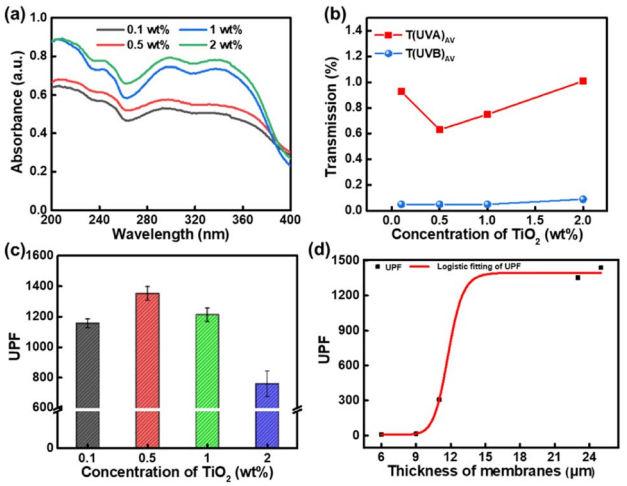

Fig. 7 UV protection performance of PAN/UV329/TiO_2 composite nanofibrous membranes with different concentrations of TiO_2: (a) UV absorption spectra, (b) $T(UVB)_{AV}$ and $T(UVA)_{AV}$, and (c) UPF value. (d) UPF value of PAN/UV329/TiO_2 nanofibrous membranes with different thicknesses.

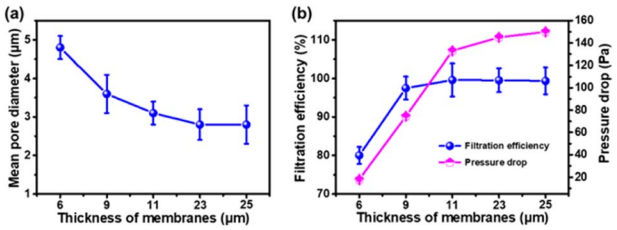

Fig. 8 (a) Mean pore diameter and (b) filtration efficiency and pressure drop of PAN/UV329-1/TiO_2-0.5 composite nanofibrous membranes with different thicknesses.

are not linearly dependent on the TiO_2 content because the light scattering properties of the TiO_2 nanoparticles are dependent on both the individual particle and cluster sizes.[35] Large flocs of TiO_2 nanoparticles scatter less light than well-dispersed TiO_2 nanoparticles. A higher TiO_2 content induces aggregation of the TiO_2 nanoparticles, lowering the light scattering efficiency. The main UV shielding modes of the TiO_2 nanoparticles are absorption and scattering: at short-wavelength UV, absorption is the main shielding mechanism; at longer wavelengths, the dominant mode is scattering.

The thickness of the nanofibrous membranes could also play a vital role in UV protection performance. Thus, with the UV329 content fixed at 1 wt% and the TiO_2 content at 0.5 wt%, the influence of the thickness on the UV protection performance was also explored (Fig. 7d). When the thickness increased from 6 to 25 μm, the UPF increased from 8 to 1439, presenting a nonlinear fitting growth trend. For thickness values up to 11 μm, the voids in the membranes were large, the UV transmittance was high and the UPF was relatively small. When the membrane thickness was increased from 11 to 25 μm, the UPF increased greatly, from 308 to 1439. When the thickness reached 25 μm, excellent UV protection performance was observed. To further evaluate the performance of the prepared PAN/UV329/TiO_2 nanofibrous membranes, their UPF values were quantitatively compared with those reported in previous recent studies.[14–16,36] In this comparison, our membranes exhibited superior UV resistance properties (Fig. S2†).

Furthermore, window air filters that protect indoor air quality from ultrafine particulate matter present in outdoor air are gaining in popularity. Because these filters are installed outside the windows or on the window screen guards, they require high UV resistance properties. Therefore, the air filtration performance of PAN/UV329-1/TiO_2-0.5 composite nanofibrous membranes with different thicknesses was also assessed, as shown in Fig. 8. Upon increasing the thickness from 6 to 25 μm, the mean pore size of the membranes decreased from 4.8 to 2.8 μm (Fig. 8a). The increasing thickness also brought about increasingly more nanofiber content in the unit area, thus improving the separation and trapping effect of the particles.[37] As displayed in Fig. 8b, when the thickness increased from 6 to 11 μm, the filtration efficiency improved from 80% to 99.62%, and the pressure drop increased from 18 to 133 Pa. Further increasing the thickness to 25 μm, the filtration efficiency remained unchanged and the pressure drop increased slightly. Thus, the proposed PAN/UV329/TiO_2 membranes are suitable for practical application in window air filters.

The influence of UV329 and TiO_2 nanoparticles on the filtration properties was investigated, as shown in Table S1.† The addition of the UV329 and TiO_2 nanoparticles endowed the membranes with increased fiber diameter and pore size, which reduced the separation and trapping effect on the particles in the polluted air. So, the filtration performance decreased with the lower efficiency. Therefore, the additives affect the filtration properties of the as-prepared membranes.

Conclusions

In summary, UV-proof PAN/UV329/TiO_2 nanofibrous membranes were fabricated effectively using one-step electrospinning. The use of UV329 as an organic UV absorber and TiO_2 nanoparticles as an inorganic UV blocker provided the membranes with double UV-resistant function. The impacts of different contents of UV329 and TiO_2 nanoparticles on the morphology and comprehensive performance of the nanofibrous membranes were investigated. When the UV329 content was adjusted to 1 wt% and the TiO_2 content was fixed at 0.5 wt%, the resulting membranes presented moderate tensile strength (7.6 MPa) and excellent UPF (1352). Moreover, the filtering performance of the PAN/UV329/TiO_2 membranes demonstrated their practical applicability in window air filters. This fabrication of such membranes could provide a facile and environmentally friendly route by which to manufacture novel materials. The PAN/UV329/TiO_2 membranes could be utilised in various other fields, such as outdoor protective clothing and window air filters.

Conflicts of interest

There are no conflicts to declare.

Acknowledgements

This work was supported by funding from the National Natural Science Foundation of China (No. 51803075 and 21704034), the Zhejiang Provincial Natural Science Foundation of China (No. LY20E030010 and TGC23B050022), and the National Innovative Training Program for College Students (No. 202010354011).

Notes and references

1 J. H. Xu, Q. J. Liang, Z. J. Li, V. Y. Osipov, Y. J. Lin, B. H. Ge, Q. Xu, J. F. Zhu and H. Bi, *Adv. Mater.*, 2022, **34**, 2200011.
2 M. Kneissl, T. Y. Seong, J. Han and H. Amano, *Nat. Photonics*, 2019, **13**, 233.
3 A. Takahashi and T. Ohnishi, *Biol. Sci. Space*, 2004, **18**, 255.
4 N. D. Paul and D. Gwynn-Jones, *Trends Ecol. Evol.*, 2003, **18**, 48.
5 A. K. Dhar and J. Koh, *Fibers Polym.*, 2021, **22**, 382.
6 O. K. Alebeid and T. Zhao, *J. Text. Inst.*, 2017, **108**, 2027.
7 D. N. Syed, M. I. Khan, M. Shabbir and H. Mukhtar, *Curr. Drug Targets*, 2013, **14**, 1128.
8 A. Yadav, V. Prasad, A. A. Kathe, S. Raj, D. Yadav, C. Sundaramoorthy and N. Vigneshwaran, *Bull. Mater. Sci.*, 2006, **29**, 641.
9 S. B. Zhang, X. H. Yang, B. Tang, L. J. Yuan, K. Wang, X. Y. Liu, X. L. Zhu, J. N. Li, Z. C. Ge and S. G. Chen, *Chem. Eng. J.*, 2018, **336**, 123.
10 Q. Z. Yu and A. A. Shen, *J. Fiber Bioeng. Inf.*, 2008, **1**, 65.
11 N. Bouazizi, A. Abed, S. Giraud, A. El Achari, C. Campagne, M. N. Morshed and F. Le Derf, *Phys. E*, 2020, **118**, 113905.
12 S. Lee, *Fibers Polym.*, 2009, **10**, 295.
13 X. M. Ren, G. L. Zhao and X. N. Li, *Polyester Ind.*, 2003, **16**, 4.
14 S. Wang, W. Chen, L. Wang, J. Yao, G. Zhu, B. Guo and M. Zhang, *J. Ind. Eng. Chem.*, 2022, **108**, 449.
15 A. G. Koozekonan, M. R. M. Esmaeilpour, S. Kalantary, A. Karimi, K. Azam, V. A. Moshiran and F. Golbabaei, *J. Text. Inst.*, 2021, **112**, 946.
16 A. A. Merati, A. M. Shoushtari and J. Mirzaei, *J. Text. Inst.*, 2017, **108**, 2086.
17 M. Zhu, J. Han, F. Wang, W. Shao, R. Xiong, Q. Zhang and C. Huang, *Macromol. Mater. Eng.*, 2017, **302**, 1600353.
18 K. N. Chen, F. N. I. Sari and J. M. Ting, *Appl. Surf. Sci.*, 2019, **493**, 157.
19 S. Fang, W. Wang, X. Yu, H. Xu, Y. Zhong, X. Sui and Z. Mao, *Mater. Lett.*, 2015, **143**, 120.
20 J. Chen, Z. Yu, C. Li, Y. Lv, S. Hong, P. Hu and Y. Liu, *Macromol. Mater. Eng.*, 2022, **307**, 2200057.
21 X. Zhong, R. Li, Z. Wang, W. Wang and D. Yu, *J. Mater. Sci.*, 2019, **54**, 13322.
22 R. Yilin, Z. Huang, M. Shi, Z. Deng and C. Dong, *Plast., Rubber Compos.*, 2022, **51**, 163.
23 W. Shao, W. Yue, G. Ren, F. Liu, F. Li, K. Weng, M. Y. Li, Y. K. Chen, T. Lu, J. P. Xiong, W. J. Bu, L. D. Wang and J. X. He, *J. Fiber Sci. Technol.*, 2020, **76**, 183.
24 J. Sheng, Y. Li, X. Wang, Y. Si, J. Yu and B. Ding, *Sep. Purif. Technol.*, 2016, **158**, 53.
25 K. Liu, L. Deng, T. Zhang, K. Shen and X. Wang, *Ind. Eng. Chem. Res.*, 2020, **59**, 4447.
26 Y. Wang, H. Wang, X. Li, D. Liu, Y. Jiang and Z. Sun, *J. Nanomater.*, 2013, **2013**, 4.
27 A. Kocić, M. Bizjak, D. Popović, G. B. Poparić and S. B. Stanković, *J. Clean. Prod.*, 2019, **228**, 1229.
28 P. Sundell and F. Sundholm, *J. Appl. Polym. Sci.*, 2004, **92**, 1413.
29 Y. Zhang, L. Yu, S. Ke, B. Shen, X. Meng, H. Huang and H. L. W. Chan, *J. Sol-Gel Sci. Technol.*, 2011, **58**, 326.
30 P. S. Kumar, K. Venkatesh, E. L. Gui, S. Jayaraman, G. Singh and G. Arthanareeswaran, *Environ. Nanotechnol., Monit. Manage.*, 2018, **10**, 366.
31 J. Liu, P. Zhou, L. Zhang, Z. Ma, J. Liang and H. Fong, *Carbon*, 2009, **47**, 1087.
32 H. Wan, N. Wang, J. Yang, Y. Si, K. Chen, B. Ding, G. Sun, M. El-Newehy, S. S. AlDeyab and J. Yu, *J. Colloid Interface Sci.*, 2014, **417**, 18.
33 N. Abidi, E. Hequet, S. Tarimala and L. L. Dai, *J. Appl. Polym. Sci.*, 2007, **104**, 111.
34 L. E. McNeil and R. H. French, *Acta Mater.*, 2000, **48**, 4571.
35 K. Nelson and Y. L. Deng, *J. Colloid Interface Sci.*, 2008, **319**, 130.
36 Y. Xu, J. Sheng, X. Yin, J. Yu and B. Ding, *J. Colloid Interface Sci.*, 2017, **508**, 508.
37 N. Wang, Z. G. Zhu, J. L. Sheng, S. S. Al-Deyab, J. Y. Yu and B. Ding, *J. Colloid Interface Sci.*, 2014, **428**, 41.